Unusual structural effects of intermolecular π-bonding in the tetracyanopyrazine (ion-radical) dimer†

Sergiy V. Rosokha,* Jianjiang Lu, Bing Han and Jay K. Kochi

Received (in Gainesville, FL, USA) 25th July 2008, Accepted 3rd October 2008
First published as an Advance Article on the web 24th November 2008
DOI: 10.1039/b812829d

The facile reduction of tetracyanopyrazine (**TCP**) by tetrakis(dimethylamino)ethylene (**TDAE**) leads to black crystals of the donor/acceptor salt: $\mathbf{TDAE}^{2+}\cdot(\mathbf{TCP})_2^{2-}\cdot 2CH_3CN$ in which the vertical anionic **TCP** stacks consisting of distinct π-$(\mathbf{TCP})_2^{2-}$ units are surrounded by **TDAE** dications. The monomers within these supramolecular π-$(\mathbf{TCP})_2^{2-}$ complexes are arranged co-facially at interplanar separation of ~3.17 Å characteristic for ion-radical π-dimers and show unusual ~30° rotation relative to each other. The structural scrutiny of the π-dimers together with the X-ray crystallographic analysis of the neutral tetracyanopyrazine acceptor, its charge-transfer complexes, and the monomeric anion-radical $\mathbf{TCP}^{-\bullet}$ reveals the unique "quasi-quinonoidal" distortion of the π-bonded tetracyanopyrazine moieties. In contrast to the molecular bending and intermolecular charge-transfer that are commonly observed in various ion-radical π-dimers and in conventional donor/acceptor complexes, the specific electron density redistribution and bond length alternation in π-bonded (planar) tetracyanopyrazine moieties (relative to the neutral molecule and isolated anion-radical) can only be accommodated by the bonding molecular orbital (HOMO) of the $(\mathbf{TCP})_2^{2-}$ dimer that is notably different from the corresponding SOMO of the monomeric $\mathbf{TCP}^{-\bullet}$.

1. Introduction

Since the discovery of tetracyanoquinodimethane and tetracyanoethylene-based organic molecular conductors[1] and magnets,[2] the anion-radical and charge-transfer salts of electron-poor polycyano-substituted acceptors have represented a major focus of organic material science, and their study have afforded rich information on the intermolecular stacking interactions extant between organic ion-radicals that are critical for various solid-state applications.[3,4] Importantly, the structural and spectral characterization of tetracyanoethylene anion-radical π-dimer $(\mathbf{TCNE})_2^{2-}$ has provided the critical experimental basis for the recent development of the concept of multi-centered long-distance intermolecular π-bonding.[5] In fact, such bonding types of π-radical/π-radical interactions that occur with interplanar separations near the limit of their van der Waals separations can be recognized in many other ion-radical salts.[6–10] The proper understanding of the nature of such unconventional bonding, as well as its thermodynamics, structural and spectral effects, and most importantly, their role in chemical reactivity[6] require the further experimental and theoretical analysis of various ion–radical associations.[5]

The availability of a variety of polycyano-substituted acceptors facilitates the preparation of novel charge-transfer and ion-radical salts and offers a unique opportunity for the development of the fundamental chemical concepts involved in long-distance bonding, in the further elucidation of π-radical stacking, as well as for the crystal engineering of new substances for material science applications. Tetracyanopyrazine (**TCP**) represents an interesting heteroaromatic acceptor for such studies because it is a π-electronic system possessing a reversible reduction potential of −0.22 V *vs.* SCE which is approximately midway between that of tetracyanoethylene and tetracyanobenzene.[11] Similar to other organic π-acceptors, **TCP** reversibly forms charge-transfer complexes with a variety of aromatic donors in solution.[12] Remarkably, the reaction of tetracyanopyrazine with vanadium hexacarbonyl has recently led to the discovery of a new type of molecular magnet,[13] and the structural and spectral characterization of **TCP** complexes with simple halide salts provide vital experimental data for the study of anion-π interactions.[14]

In this study, we carry out the structural characterizations of the **TCP** acceptor as well as its anion-radical and charge-transfer salts, which provide new and important information on the nature and properties of long-distance ion-radical π-bonding.

Department of Chemistry, University of Houston, 4800 Calhoun Rd., Houston, TX 77204, USA. E-mail: srosokha@uh.edu; Fax: +1-713-743-2709; Tel: +1-713-743-3292

† Electronic supplementary information (ESI) available: Unit cell of the tetracyanopyrazine (**TCP**) crystal (Fig. S1); electronic spectrum of $\mathbf{TCP}^{-\bullet}$ anion-radical (Fig. S2); structures of **TCP** complexes with tetrathiafulvalene, biphenylene and pyrene (Fig. S3); ion-radical π-associations *via* the bonding combination of their SOMOs for **TCNE**, naphthalene and *p*-chloranil radicals (Fig. S4); SOMO of ion radicals and HOMO of π-dimer for **TCNE**, p-chloranil and **TCP** anion-radicals (Fig. S5); HOMO, LUMO and LUMO+1 of **TCP** (Fig. S6); HOMO of $(\mathbf{TCP})_2^{2-}$ dimer drawn with different boundary density conditions (Fig. S7), molecular structure of sigma-bonded dimer σ-$(\mathbf{TCP})_2^{2-}$ salt with $[K^+(\text{cryptand})]$ counter-ion (Fig. S8), complete ref. 30, structural comparison of monomeric and π-bonded ion-radical of **DDQ**, *p*-chloranil and ocrtamethylanthracene (Table S1). CCDC reference numbers 703968–703974. For ESI and crystallographic data in CIF or other electronic format see DOI: 10.1039/b812829d

2. Results

2.1 Structural characteristics of tetracyanopyrazine and its separated anion radical

The quantitative analysis of the anion-radical and the charge-transfer salts of tetracyanopyrazine acceptor require prior identification of the X-ray structural characteristics of the parent **TCP** acceptor and of its minimally disturbed anion radical. Since such basic information is lacking in crystallographic literature, we initially carried out X-ray measurements of the **TCP** acceptor and its monomeric anion radical salts.

2.1.1 X-Ray crystallography of the TCP acceptor. Colorless crystals of neutral tetracyanopyrazine were obtained by the slow, deliberate evaporation of its acetonitrile solution at room temperature under air. Single-crystal X-ray measurements reveal an orthorhombic unit cell in *Pbca* space group shown in Fig. S1 in ESI† (see Experimental section for crystallographic details). This cell contains eight structurally identical tetracyanopyrazine molecules that are roughly planar with mean atomic deviation from the least-square plane of ~0.03 Å. The length of the chemically equivalent bonds within **TCP** moieties are essentially invariant, their deviations from the corresponding average values being less than the accuracy of X-ray measurements ($3\sigma \approx 0.005$ Å). As such, neutral tetracyanopyrazine has approximately D_{2h} symmetry, and its average bond lengths are listed in Table 1.

2.1.2 Crystallographic and spectral characterization of the monomeric tetracyanopyrazine ion-radical. To prepare single crystals of **TCP** anion-radical salts, we first turned to the alkali-metal reduction of the neutral parent in the presence of crown-ether ligands based on our earlier reduction studies of various acceptors.[15] The potassium-mirror reduction of tetracyanopyrazine in THF in the presence of dicyclohexano-18-crown-6 (L) followed by slow diffusion of hexane into the resulting brown solution (at −30 °C) led to yellow crystals suitable for crystallographic study; and their X-ray analysis

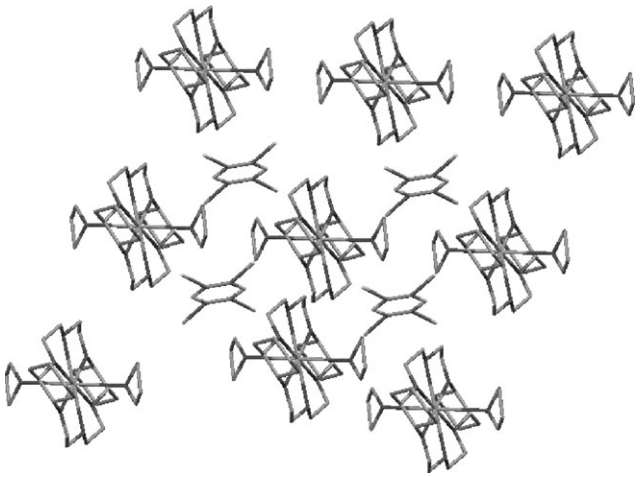

Fig. 1 Crystal lattice of $[K(L)(THF)_2]$(**TCP**) salt.

revealed the triclinic unit cell in $P\bar{1}$ space group. The crystal lattice (Fig. 1) is dominated by the bulky complexes of potassium cations with equatorially coordinated crown ether ligands and a pair of THF solvent molecules in axial positions. The voids between these quasi-spherical complexes are occupied by **TCP** moieties. As a result of such a crystal packing, the tetracyanopyrazine anion-radicals are well-separated from each other and from the potassium cations (encapsulated by a lipophilic coordination shell) and are thus minimally disturbed by interionic electrostatic forces.[15] The tetracyanopyrazine anion-radical is centrosymmetric and essentially planar. Its quantitative comparison with neutral **TCP** in Table 1 reveals that the addition of a single electron results in a noticeable increase (~0.03 Å) of the C_{Ar}–N_{Ar} aromatic bond lengths (α/α'). On the other hand, the C_{Ar}–C_{Ar} (γ) and C_{Ar}–C_{CN} (β/β') bonds of the anion-radical are somewhat shorter than those in the neutral acceptor, but the differences (~0.015 Å) are less pronounced than that observed for the α bond lengths. Finally, the C≡N bond lengths are essentially the same as those in the neutral acceptor. Most importantly, such a bond length analysis reveals that the structure of the

Table 1 Structural characteristics of various tetracyanopyrazine moieties[a]

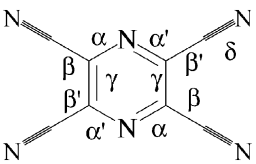

		α/α'[b]	β/β'[b]	γ	δ
TCP		1.331 ± 0.002	1.447 ± 0.003	1.405 ± 0.002	1.141 ± 0.002
$\mathbf{TCP}^{-\bullet}$[c]		1.359 ± 0.004	1.433 ± 0.004	1.388 ± 0.002	1.144 ± 0.003
$(\mathbf{TCP})_2^{2-}$[d]	A	1.332 ± 0.005/1.377 ± 0.003[e]	1.449 ± 0.004/1.434 ± 0.003[e]	1.399 ± 0.005	1.148 ± 0.005
	B	1.329 ± 0.005/1.377 ± 0.003[e]	1.454 ± 0.006/1.427 ± 0.007[e]	1.406 ± 0.004	1.141 ± 0.008
[**TTF**,**TCP**][f]		1.337 ± 0.002	1.446 ± 0.004	1.407 ± 0.002	1.143 ± 0.002
[**BP**,**TCP**][g]		1.332 ± 0.002	1.443 ± 0.002	1.409 ± 0.002	1.151 ± 0.002
[**PYR**,**TCP**][h]		1.332 ± 0.002	1.447 ± 0.004	1.405 ± 0.002	1.142 ± 0.003

[a] Values of average bond lengths and their deviations, in Å (see Experimental section). [b] $\alpha = \alpha'$ and $\beta = \beta'$ unless noted otherwise. [c] In $[K(L)(THF)_2]$ **TCP** salt, L = dicyclohexano-18-crown-6. [d] In **TDAE**·$(\mathbf{TCP})_2$·$2CH_3CN$ salt, A and B represent two independent **TCP** moieties, **TDAE** = tetrakis(dimethylamino)ethylene. [e] (f) $\alpha \neq \alpha'$ and $\beta \neq \beta'$. [f] **TTF** = tetrathiafulvalene. [g] **BP** = biphenylene. [h] **PYR** = pyrene.

monomeric anion radical retains approximately D_{2h} symmetry, similar to that in the neutral acceptor.

The ESR spectrum of the yellow solution of the crystalline [K(L)(THF)$_2$](**TCP**) salt dissolved in tetrahydrofuran accords with that reported earlier for **TCP**$^{-\bullet}$ anion radical obtained by the reduction of tetracyanopyrazine with metallic thallium,[11] and it is characterized by well-resolved hyperfine splittings from the aromatic and cyano groups nitrogens: $a(2N_{ar})$ = 3.8 G and $a(4N_{CN})$ = 0.62 G, respectively. The electronic spectrum of this solution shows a strong, sharp absorption band at λ_{max} = 483 nm ($\log\varepsilon$ = 3.8) and a weaker band at 453 nm (Fig. S2 in ESI†).

2.2 Structural characterization of the π-dimers of tetracyanopyrazine

2.2.1 Preparation and structural identification of π-bonded tetracyanopyrazine dyads. The strong organic donor: tetrakis-(dimethylamino)ethylene (**TDAE**) is characterized by a pair of one-electron oxidation potentials at E^{o}_{ox} = −0.68 V and −0.53 *vs.* SCE,[16] which are both more negative than the reduction potential of the **TCP** acceptor (*vide supra*). Accordingly, the addition of a small amount of **TDAE** to a colorless 10 mM solution of tetracyanopyrazine in acetonitrile results in its spontaneous reduction, and the UV-Vis spectrum of this yellow solution contains well-resolved absorption bands at 453 and 483 nm, characteristic of the **TCP**$^{-\bullet}$ anion-radical. Their spectral intensities indicate the formation of 2 moles of anion-radical for each mole of added donor. On the other hand, when the acetonitrile solution that contains **TDAE** donor together with two equivalents of **TCP** acceptor is cooled to −35 °C, an additional broad absorption band at λ_{max} ~ 550 nm appears, and a black crystalline material precipitates soon thereafter (see Experimental section for details). The single-crystal X-ray analysis reveals an orthorhombic unit cell in *Pbca* space group. The crystal lattice consists of vertical stacks of tetracyanopyrazines separated by the molecules of **TDAE** and solvent, with overall stoichiometry: **TDAE**·(**TCP**)$_2$·2CH$_3$CN as illustrated in Fig. 2A.

The **TCP** columns show distinct dimeric units consisting of two crystallographically independent tetracyanopyrazine moieties (A and B in Table 1) which are cofacially stacked atop each other at an interplanar separation of r_{DA} = 3.17 Å. Such an intimate pairing leads to multiple interatomic contacts that are all significantly shorter than the sum of their van der Waals radii (identified by the light grey lines in Fig. 2B). By comparison, the average inter-dimer separations in these columns are roughly 3.50 Å; and the distances between atoms of neighboring dimers are >0.1 Å greater than the sum of the van der Waals radii. Further inspection of the dimeric units reveals that the tetracyanopyrazine planes are nearly parallel within each pair, but one of the moieties is rotated by 36° relative to the other (Fig. 2B). As a result, the core atoms of one molecule are located over the middle of the bond of its counterpart.

2.2.2 Charge distribution in TDAE·(TCP)$_2$·2CH$_3$CN salt. For the evaluation of the charge residing on the π-(**TCP**)$_2$ dyads, we considered the structural characteristics of the **TDAE** moiety by following the earlier report by Miller and co-workers.[16a] In this regard, the central C–C bond length of 1.513 Å in **TDAE** moiety measured in the **TDAE**·(**TCP**)$_2$·2CH$_3$CN salt corresponds to that reported earlier for the **TDAE**$^{2+}$ dication, and it is significantly longer than the values of 1.36 and 1.42 Å that are characteristic of the neutral donor (**TDAE**) and the monocation (**TDAE**$^{+}$), respectively.[16] Furthermore, the IR measurements of **TDAE**·(**TCP**)$_2$·2CH$_3$CN reveals a doublet C–N stretching bands at 1658 and 1666 cm^{-1} that is also characteristic of **TDAE**$^{2+}$ (as compared with the bands at 1340 cm^{-1} and at 1518 cm^{-1} measured for the neutral donor and the monocation, respectively).[16] Accordingly, we conclude that the **TDAE**·(**TCP**)$_2$·2CH$_3$CN crystals consist of the **TDAE**$^{2+}$ dication, and its double positive charge is balanced by the dianionic (**TCP**)$_2^{2-}$ dyad. Moreover, the structural similarity of the two independent tetracyanopyrazines (identified as A and B in Table 1) points to the approximately equal charge residing on each **TCP** moiety. Comparison of the average bond lengths of the π-dimeric tetracyanopyrazine moieties (*e.g.* C_{Ar}–N_{Ar} bond length of 1.354 Å) also supports their overall anionic charge. However, we realize that relatively minor structural differences between neutral tetracyanopyrazine and its anion radicals (see Table 1) may hinder a reliable independent evaluation of charge residing on tetracyanopyrazine based solely on its structural features, especially in the **TDAE**·(**TCP**)$_2$·2CH$_3$CN salt, in which the **TCP** moieties are notably less symmetric (*vide infra*).

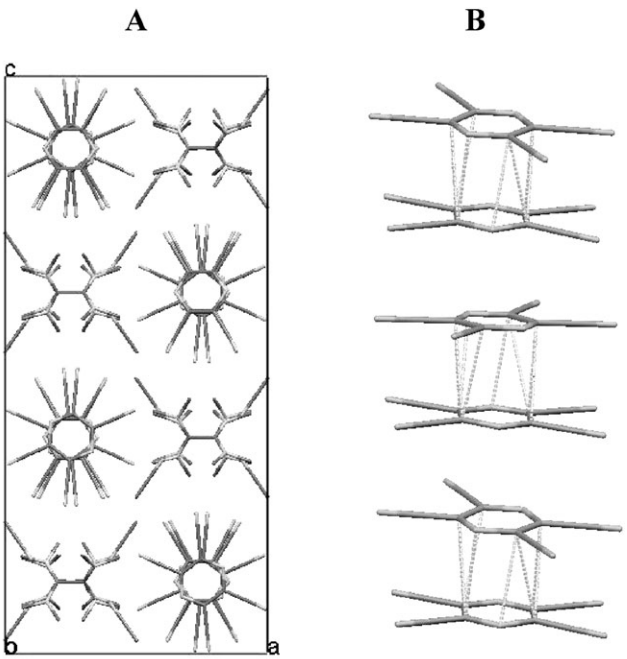

Fig. 2 (A) View of the crystal lattice (along the *b* axes) of the **TDAE**·(**TCP**)$_2$·2CH$_3$CN salt. (B) Tetracyanopyrazine stacks with light grey lines that denote contacts shorter then van der Waals separations.

2.2.3 The structural features of π-bonded tetracyanopyrazine. Although the two **TCP** moieties designated as A and B within each dimer are crystallographically independent, their structural features are essentially the same within the accuracy

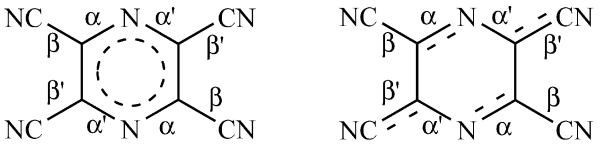

Monomeric TCP$^{\cdot-}$ ($\alpha = \alpha'$, $\beta = \beta'$) π-Bonded TCP$^{\cdot-}$ ($\alpha \neq \alpha'$, $\beta \neq \beta'$)

Chart 1

of X-ray measurements (Table 1). Most notably, each of the π-bonded **TCP** moieties is distorted, in contrast to the roughly D_{2h}-symmetry that characterize neutral tetracyanopyrazine and its monomeric anion-radical. Indeed, each of the A and B units within the $(\mathbf{TCP})_2^{2-}$ π-dimer show two pairs of *markedly different* aromatic C_{Ar}–N_{Ar} bonds: α = 1.33 Å and α' = 1.38 Å. Furthermore, the C_{Ar}–C_{CN} bond lengths within each π-bonded tetracyanopyrazine also vary somewhat: β = 1.45 Å and β' = 1.43 Å (Table 1). As a result, their structural features can be visualized as a "quasi-quinonoidal" distortion, as pictorially illustrated in Chart 1 (somewhat exaggerated, for clarity).

By comparison, the variations of the other bond lengths (γ and δ) within each π-bonded moiety are insignificant (*i.e.*, the differences between the chemically equivalent bond lengths are within the accuracy of the X-ray measurements). Nonetheless, variations of the formally equivalent α *versus* α' and β *versus* β' bonds are sufficient to decrease the symmetry of these molecules to roughly C_{2h} relative to the approximately D_{2h} characteristic of the neutral acceptor and its monomeric anion radical (*vide supra*).

2.3 Structural characterization of the charge-transfer complexes of tetracyanopyrazine

In view of the unusually pronounced bond variations within the π-bonded tetracyanopyrazine dianionic dimer, we prepared single crystals and carried out X-ray studies of charge-transfer complexes of this acceptor with several conventional organic donors: tetrathiafulvalene (**TTF**), biphenylene (**BP**) and pyrene (**PYR**) to represent typical examples of intermolecular bonding. In all cases, alternating donor/acceptor stacks were observed (Fig. S3 in ESI†), and the interplanar separations (r_{DA}) were typical of 1 : 1 charge-transfer complexes; *i.e.* r_{DA} = 3.33, 3.29 and 3.35 Å for [**TTF**, **TCP**], [**BP**, **TCP**] and [**PYR**, **TCP**], respectively. The tetracyanopyrazine structures extant in all of these diverse complexes are quite similar to that of the parent **TCP** acceptor (Table 1), and this consistent invariance points to the minor degree of donor/acceptor charge transfer. Nevertheless, in [**TTF**, **TCP**] containing the extremely strong tetrathiafulvalene donor (**TTF**),[7b] the central C=C bond length of 1.359 Å and adjusted C–S bond length of 1.754 Å on the **TTF** moiety suggest that some charge transfer (roughly to ~0.1) may pertain.[17] However, most pertinent to the current study is the fact that the tetracyanopyrazine moieties are characterized by approximately D_{2h} symmetry in all of these complexes, and this again underscores the unique character of the "quasi-quinonoidal" distortion resulting from the long-distance bonding in the π-dimer $(\mathbf{TCP})_2^{2-}$.

3. Discussion

The X-ray crystallography of the salts resulting from reduction of the tetracyanopyrazine acceptor with **TDAE** donor reveals the presence of distinct π-bonded $(\mathbf{TCP})_2^{2-}$ dyads, which show two remarkable structural features. First, an unusual ~30° rotation of one tetracyanopyrazine moiety relative to its counterpart. Second, a significant "quasi-quinonoidal" distortion of each monomeric unit. Such notable structural characteristics are quite unique for the ion-radical π-dimers, and they appear to be closely related to the properties of the frontier orbitals of monomeric and dimeric species. Accordingly, let us now concentrate in the following discussion on the structural analysis of $(\mathbf{TCP})_2^{2-}$ dyads together with the quantum mechanical evaluation of their frontier molecular orbitals (*via* single-point HF/6-311G* computations, see Experimental section for details), sufficient to provide new insight into the nature and properties of the intermolecular π-bonding. As such, the quantitative evaluation of the energetics of the unique long-distance interaction (which underlies their common for π-dimer interplanar separation of ~3.17 Å) and detailed discussion of its components (*i.e.* electron correlation, electrostatics, *etc*,[9,10,18–20]) will be deferred.

3.1 Molecular orbital background for the stacking geometry of the π-dimer $(\mathbf{TCP})_2^{2-}$

While the analysis of the energetics of dimer formation requires high-level computations and involves specific consideration of electron correlations and electrostatics,[9,10,19,20] the recently reported approach[18] based on interplay between frontier orbital bonding and hard-core repulsion appears as useful method of the clarification of monomer arrangements (in the analogous way as the Woodward–Hoffman rules govern reaction pathways).[21] Indeed, Fig. S4 in ESI† illustrates the (frontier) molecular orbital origin of the fully eclipsed stacking in tetracyanoethylene dimer $(\mathbf{TCNE})_2^{2-}$,[5] the lateral shift in the π-dimers of the p-chloranil anion-radicals,[7] and the 90° turn in the π-association of naphthalene cation-radicals.[22a] Similarly, the SOMO shapes determine the rotation of the stacked monomers by the 60° in the dimer of phenalenyl radicals,[19] by the 180° in fluoranthrene cation-radical π-associates,[22b] and various stackings of tetrathiafulvalene[7b] and thianthrene cation-radicals.[23]

The SOMO of $\mathbf{TCP}^{-\bullet}$ anion-radical (see Experimental section for computational details) is located mostly on the aromatic carbons. Its shape is shown in Fig. 3(left), and its symmetry indicates that fully eclipsed arrangements of $\mathbf{TCP}^{-\bullet}$ monomers atop each other leads to an antibonding orbital overlap (in contrast, *e.g.* to bonding combination of SOMOs of $\mathbf{TCNE}^{-\bullet}$ in Fig. S4A). Furthermore, the 60° turn of one of the **TCP** moieties, as implied by the hexagonal **TCP** core, lead the bonding orbital overlap between only two pairs of carbons atoms. In such a conformation, however, the other core carbons would lie over the nitrogens with no bonding orbital overlap. Furthermore, such a 60° turn maximizes the core-electron repulsion of all the aromatic atoms. Thus, the 36° rotation of monomers found in $(\mathbf{TCP})_2^{2-}$ π-dimer represents an energetically favorable midway between two

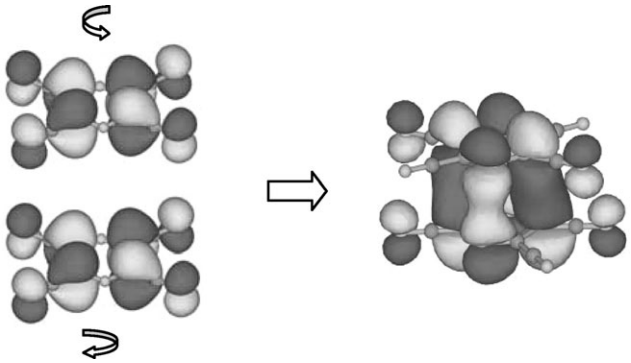

Fig. 3 Illustration of the π-bonding of tetracyanopyrazine anion-radicals.[24]

limiting arrangements (*i.e.* 0 and 60° turns), in qualitative agreement with the "maximin" principle.[18] Importantly, the Gaussian HF/6-311G* computations (see Experimental section for details) also shows energy minimum when one monomer is rotated ~37° relative to another (Fig. 4)[24]

3.2 Structural effects of the long-distance π-bonding

In accord with conventional MO diagram, the SOMO orbitals of anion-radicals combine to generate bonding (HOMO) and antibonding (LUMO) orbitals of dianionic π-dimer.[5,7,20] Such a diagram for $(\mathbf{TCP})_2^{2-}$ dyad is presented in Fig. 5 together with the HOMO/LUMO shapes obtained *via* single-point Gaussian 98 computations of this dimer (see Experimental section).[24c]

Cursory glance at the orbital shapes in Fig. 3 and 5 reveals qualitative resemblance between the dimer's HOMO and the pair of SOMOs of monomers turned ~30° relative to each other (and this implies that the linear combination of a $\mathbf{TCP}^{-\bullet}$ SOMOs represent major contribution to HOMO/LUMO of $(\mathbf{TCP})_2^{2-}$ dyad). The close scrutiny of the HOMO shape of the π-$(\mathbf{TCP})_2^{2-}$ dimer in Fig. 6B, however, reveals that each bonding fragments of the HOMO is delocalized over four atoms: *viz.*, the C_{Ar}–N_{Ar} pair on one monomer and the

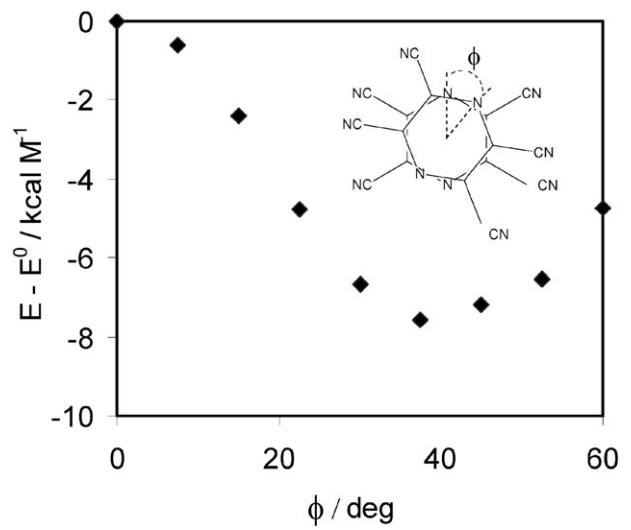

Fig. 4 Dependence of the energy of the diamagnetic $(\mathbf{TCP})_2^{2-}$ dimer on the lateral rotation of one monomer relative to another.

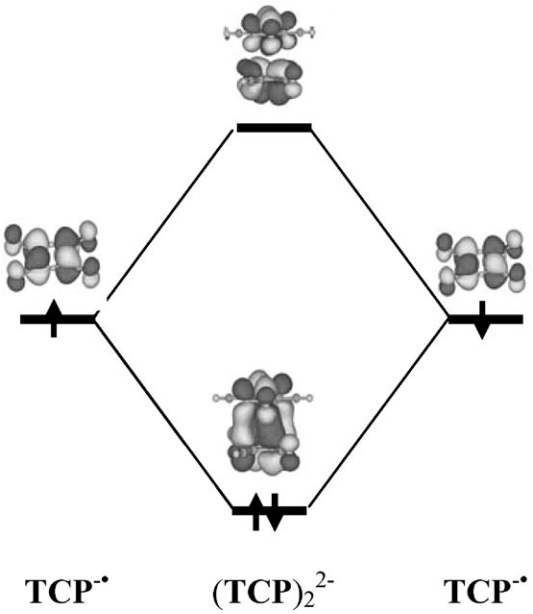

Fig. 5 Simplified molecular orbital diagrams of the $(\mathbf{TCP})_2^{2-}$ dimer.

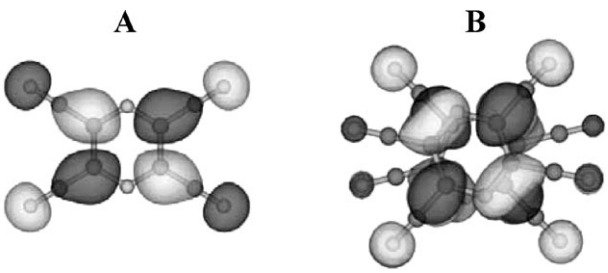

Fig. 6 Top view of (A) the SOMO of the $\mathbf{TCP}^{-\bullet}$ anion-radical (bonding relative to four C_{Ar}–C_{CN} fragments) and (B) the HOMO of the $(\mathbf{TCP})_2^{2-}$ dimer (bonding relative two C_{Ar}–N_{Ar} and two C_{Ar}–C_{CN} fragments in each monomer).

C_{Ar}–C_{CN} pairs on the other (see side and top views in Fig. 3 and 6, respectively). In other words, the core atoms of one monomer arranged over the center of the aromatic bond of its counterparts, and the "bonding" fragments of its HOMO envelop the perpendicularly-aligned C_{Ar}–N_{Ar} and C_{Ar}–C_{CN} bonds of the constituent pair of monomers. Notably, such a shape noticeably deviate from that of the monomeric anion-radical of tetracyanopyrazine, which is symmetrically bonding relative to the four C_{Ar}–C_{CN} bonds. Thus, π-bonding of tetracyanopyrazine anion-radicals (which occur at ~30° relative rotation of monomers) results in formation of dimer's HOMO which, in addition to combination of monomer SOMOs, probably contains significant contribution of their lower and/or upper laying orbitals (see HOMO, LUMO and LUMO + 1 of neutral tetracyanopyrazine in Fig. S5 in ESI†).[24]

The calculated shape of the bonding orbital of π-$(\mathbf{TCP})_2^{2-}$ in Fig. 6 is closely related to the "quasi-quinonoidal" distortion of the π-bonded tetracyanopyrazine moiety illustrated in Chart 1 (right). Indeed, the top view of the HOMO in Fig. 6 indicates that it is bonding with respect to two C_{Ar}–N_{Ar} (α) bonds and antibonding with respect to another pair of C_{Ar}–N_{Ar} (α′) bonds within each monomer. Thus, the electron

population of this orbital is expected to preferentially elongate the α' bonds.[9b,25] Indeed, such a prediction agrees well with the experimental bond lengths of α = 1.33 Å and α' = 1.38 Å of the π-bonded anionic tetracyanopyrazine moiety in π-(**TCP**)$_2^{2-}$ (compare: $\alpha = \alpha'$ = 1.33 Å in **TCP** and $\alpha = \alpha'$ = 1.36 Å in monomeric **TCP**$^{-\bullet}$). In a similar way, the HOMO of the π-(**TCP**)$_2^{2-}$ is bonding with respect to only two of C_{Ar}–C_{CN} bonds (β') within each tetracyanopyrazine moiety, and its population is thus expected to affect the β and β' bonds differently. This prediction also accords well with X-ray measurements which afford: β = 1.45 Å and β' = 1.43 Å for π-bonding of tetracyanopyrazine in π-(**TCP**)$_2^{2-}$, in contrast to uniform values $\beta = \beta'$, which are observed in both neutral **TCP** and monomeric **TCP**$^{-\bullet}$ anion-radical.

It must also be stressed that the formation of the ion-radical π-dimer is frequently accompanied by the molecular bending of the monomeric moieties.[7,8] Such a distortion (relative to their separated monomeric analogues) is related to the fact that the π-bonding interaction involves only a fraction of the ion-radical moiety. Thus, the interplay between the attraction that is concentrated on one fragment and the steric repulsion between the remaining parts leads to bending of the π-bonded species. For example, in the π-dimer of *p*-chloranil anion-radical,[7] the oxygen atoms which are involved in the bonding HOMO of the dimer are clearly bent toward each other (see Fig. S4 in ESI†), whereas the non-bonding chlorine substituents are noticeably bent in the *opposite* direction. A different type of structural effects of the π-dimerization were observed with complex radical species consisting of the two (bridged) phenalenyl units.[9b,10c] For example, intermolecular π-bonding of one of phenalenyl fragment in a spiro-bis(1,9-disubstituted-phenalenyl)boron radicals resulted in a electron-density shift from those fragments which are not directly involved in the π-dimer interactions to units directly involved in π-bonding, and, thus, the geometries of these fragments became different.[9b] In another biphenalenyl biradicaloid, the noticeable geometry changes of dimerized species (relative to isolated monomers) were related to partial localization of the SOMO electrons accompanying intermolecular π-bonding (which made them less available for the intramolecular delocalization).[10c] In comparison, our analysis of the structural data on the various π-dimers of relatively simple ion-radicals (other than the **TCP**) indicates that bond length distributions within π-bonded moieties are close to those in monomers (and a similarity of bond lengths accords with the fact that the SOMO shape of the ion-radicals and HOMO of the π-dimers are essentially the same when viewed perpendicular to the molecular plane, see Fig. S6 in ESI†).[26]

The "quasi-quinonoidal" distortion of the tetracyanopyrazine moieties reported herein represents quite a unique effect of the long-distance π-bonding. Such a structural alteration (arising from the change in electron density distribution) is specific and it cannot be explained by either steric effects or partial charge transfer (intermolecular or between more or less distinct fragments of complex radical). However, distortion arises naturally from the consideration of the bonding HOMO of the π-dimers, the shape of which is significantly different from that of the SOMO of the monomeric anion-radical (Fig. 3, Fig. 6, and Fig. S6†). As such, the experimental observation of the significant distinctions between the formally α- *versus* α'- and β- *versus* β'-bonds in Table 1 supports the validity of the theoretical evaluation of the bonding interaction within the π-(**TCP**)$_2^{2-}$ dimer. It also demonstrates that even at a separation between molecules of ~3.2 Å (*i.e.* near the limit of van der Waals contacts), the long-distance π-bonding is capable of very specific and non-trivial effects on the structure (and therefore the reactivity) of the counterparts.

3.3 Long-distance π-bonding in ion-radical π-dimers *versus* that in charge-transfer complexes

The delocalized intermolecular radical/radical interactions extant in π-dimers is closely related to that commonly observed in traditional donor/acceptor molecular complexes, as described by Mulliken charge-transfer theory.[27] Indeed, the experimental characteristics of π-dimers and charge-transfer complexes are strikingly akin. Structurally, both types of bimolecular associates are characterized by parallel cofacial stacking of counterparts at interplanar separations of $r_{DA} \approx 3.1 \pm 0.3$ Å. Spectral studies reveal that they are usually diamagnetic species with intense (low-energy) absorption bands related to the (bonding/antibonding) HOMO–LUMO transitions. Finally, the π-dimers and charge-transfer complexes are typically characterized in solution by formation enthalpies of $\Delta H_{DA} \approx$ 3–10 kcal mol^{-1}.[7,27]

The parallel experimental properties of both types of associates stress the similarity in the delocalized intermolecular interactions as illustrated *via* simplified molecular-orbital diagrams in Fig. 5 for typical π-dimers and charge-transfer complexes in Fig. 7.

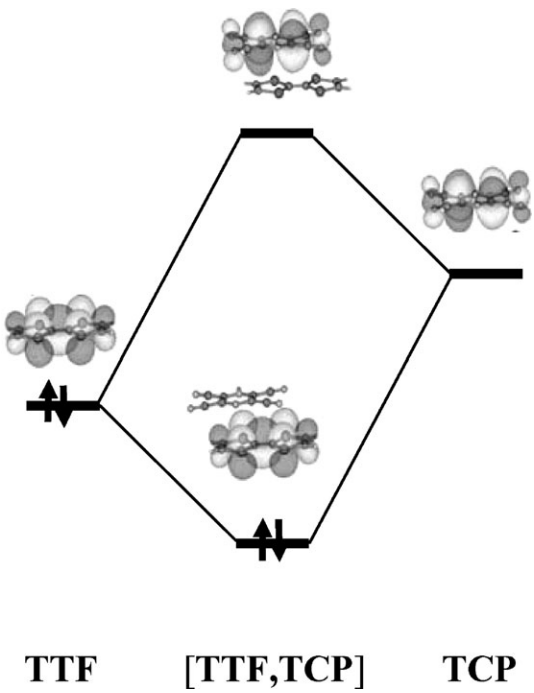

Fig. 7 Simplified molecular orbital diagrams of the charge-transfer complex [**TTF**, **TCP**].

At first glance, the two MO diagrams appear to be somewhat different. Indeed, the bonding and antibonding orbitals of the π-dimer results form the SOMO/SOMO interaction of the ion-radical and are symmetrically delocalized over both monomers (Fig. 5). In comparison, the interaction of HOMO donor with the LUMO acceptor in charge-transfer complexes leads to a bonding orbital located preferentially on the TTF donor and the antibonding orbital located on the TCP acceptor (Fig. 7). However, when either donor and/or acceptor strength is increased, their contribution to the bonding molecular orbitals of the complex become comparable, as found in *o*-chloranil complex with **TTF** and complexes of the strong nitrosonium acceptor with aromatic donors.[28] In the latter situation, the degree of the donor/acceptor charge transfer becomes quite significant. Such an increase in degree of charge transfer is accompanied by the corresponding changes in bond length, in accord with the geometries differences of the parent donor and acceptor and their cation or anion radicals. For example, charge transfer to the dichlorodicyano-*p*-benzoquinone (**DDQ**) acceptor in complexes with strong donors results in more uniform bond distribution within the **DDQ** ring (*i.e.* an increase in benzenoid character). It is important to note, however, that such structural changes can be related to partial population/depopulation of the original HOMO and LUMO of donor and acceptor and their normalized linear combination within the context of two-state Mulliken theory represents the molecular orbital of the complex.[26] By strong contrast, the structural and electronic changes in π-bonded tetracyanopyrazine moieties are related to distinctive changes in the molecular orbitals of the $(\mathbf{TCP})_2^{2-}$ π-dimer relative to that of constituent anion-radical.

4. Conclusions

The X-ray crystal structure of the dianionic π-dimer $(\mathbf{TCP})_2^{2-}$ reveals the unusual ~30° rotation of the monomeric units and the "quasi-quinonoidal" distortion of the π-bonded moieties in comparison with that in the neutral tetracyanopyrazine acceptor, its charge-transfer complexes and separated anion-radical salt. The molecular orbital calculations reveal that such structural features are related to symmetries of the frontier orbitals of monomeric *versus* those of the dimeric species. Most importantly, this study demonstrates for the first time that (a) the π-radical/π-radical interaction near the limit of van der Waals separations can effect notably the electron density distribution and molecular geometries of the relatively simple monomeric units, and (b) such changes can be accommodated by the formation of distinct molecular orbital between the species near the limit of their van der Waals separations, which is distinctively different from that of the SOMO of the monomeric ion-radical.

5. Experimental

Materials

Tetrakis(dimethylamino)ethylene, dicyclohexano-18-crown-6 and potassium metal (Aldrich) were used without additional purification. Tetracyanopyrazine was a generous gift from Dr J. F. Neumer (Du Pont Co). Tetrahydrofuran, hexane, dichloromethane and acetonitrile were purified as described earlier[15] and stored under an argon atmosphere.

Crystallization

Colorless crystals of neutral **TCP** were produced by slow evaporation of an acetonitrile solution. To obtain the crystals of separated anion-radical salt [K(L)$(THF)_2$](**TCP**), 36 mg of tetracyanopyrazine together with 50 mg of L = dicyclohexano-18-crown-6 were dissolved in 20 mL of dry THF in a Schlenk tube, and the solution was transferred (under argon) into another Schlenk tube in which potassium mirror was prepared by (*in vacuo*) heating of 10 mg of metal, as described earlier.[15] The resulting red-brown solution was layered with hexane (20 mL), cooled to −30 °C, and yellow crystals suitable for X-ray crystallography grew on the walls after several days. Note that the similar potassium mirror reduction of tetracyanopyrazine in the tetrahydrofuran solution in the presence of 2,2,2-cryptand afforded σ-bonded dianionic dimers $(\mathbf{TCP})_2^{2-}$ (see Fig. S7 in ESI†). The black crystals of (**TDAE**)$(\mathbf{TCP})_2 \cdot 2CH_3CN$ were obtained by addition of 20 mg of **TDAE** donor to a solution 36 mg of tetracyanopyrazine acceptor in 20 ml of acetonitrile (under argon protection), and slowly cooling the resulting dark-brown solution to −30 °C. The crystal of [**TTF**, **TCP**] were obtained by dissolution of 10 mg of donor and 9 mg of acceptor in 15 ml of dichloromethane (in 50 ml Schlenk tube), followed by layering the solution with 25 ml of hexane and slow cooling to −60 °C. After several days dark-green crystals were formed.

The diffraction data were collected with the aid of a Bruker SMART Apex diffractometer equipped with a CCD detector using Mo-Kα radiation (λ = 0.71073 Å), at −100 °C. The structures were solved by direct methods and refined by full matrix least-squares procedure.[29] The values of deviations σ_T in Table 1 were calculated as square root of bond length crystallographic accuracy (σ_c) and variation (σ_v), *i.e.* $\sigma_T = (\sigma_c^2 + \sigma_v^2)^{1/2}$.

TCP. Formula: C_8N_6. MW 180.14, orthorhombic *Pbca*, a = 10.090(2), b = 12.141(3), c = 13.850 (3) Å, V = 1696(6) Å^3, D_c = 1.410 g cm^{-3}, Z = 8. The total number of reflections measured were 11774 of which 2529 reflections were symmetrically non-equivalent. Final residuals were $R1$ = 0.0481 and $wR2$ = 0.1286 for 1931 reflections with $I > 2\sigma(I)$.

[K(L)$(THF)_2$](TCP). Formula: $C_{36}H_{52}KN_6O_8$. MW 735.94, triclinic, $P\bar{1}$, a = 9.743(3), b = 10.035(3), c = 11.123(3) Å, α = 81.707(5), β = 69.085(5), γ = 73.712(5)°, V = 973.8(4) Å^3, D_c = 1.255 g cm^{-3}, Z = 1. The total number of reflections measured were 14720 of which 5609 reflections were symmetrically non-equivalent. Final residuals were $R1$ = 0.0468 and $wR2$ = 0.1308 for 3497 reflections with $I > 2\sigma(I)$.

(TDAE)·$(TCP)_2$·$2CH_3CN$. Formula: $C_{30}H_{30}N_{18}$. MW 642.72, orthorhombic, *Pbca*, a = 14.971 (15), b = 13.39(2), c = 33.07(4) Å, V = 6631(16) Å^3, D_c = 1.288 g cm^{-3}, Z = 8. The total number of reflections measured were 43697 of which 9903 reflections were symmetrically non-equivalent. Final

residuals were $R1 = 0.0696$ and $wR2 = 0.1916$ for 5031 reflections with $I > 2\sigma(I)$.

[TTF, TCP]. Formula: $C_{14}H_4N_6S_4$. MW 384.47, triclinic, $P\bar{1}$, $a = 6.0656(8)$, $b = 7.8452(11)$, $c = 8.6868(12)$ Å, $\alpha = 86.475(2)$, $\beta = 75.290(2)$, $\gamma = 75.507(2)^\circ$, $V = 387.10(9)$ Å^3, $D_c = 1.649$ g cm^{-3}, $Z = 1$. The total number of reflections measured were 5845 of which 2273 reflections were symmetrically non-equivalent. Final residuals were $R1 = 0.0305$ and $wR2 = 0.0838$ for 2124 reflections with $I > 2\sigma(I)$.

[BP, TCP]. Formula: $C_{20}H_8N_6$. MW 332.32, monoclinic, $P2_1/n$, $a = 8.6134(4)$, $b = 6.9065(3)$, $c = 13.2991(6)$ Å, $\beta = 902680(10)^\circ$, $V = 781.13$ (6) Å^3, $D_c = 1.395$ g cm^{-3}, $Z = 2$. The total number of reflections measured were 3439 of which 3439 reflections were symmetrically non-equivalent. Final residuals were $R1 = 0.0423$ and $wR2 = 0.1178$ for 2926 reflections with $I > 2\sigma(I)$.

[PYR, TCP]. Formula: $C_{16}H_{10}N_6$. MW 382.38, monoclinic, $P2_1/n$, $a = 8.747(3)$, $b = 6.940(2)$, $c = 15.327(5)$ Å, $\beta = 104.356(7)^\circ$, $V = 901.4$ (5) Å^3, $D_c = 1.409$ g cm^{-3}, $Z = 2$. The total number of reflections measured were 8909 of which 2650 reflections were symmetrically non-equivalent. Final residuals were $R1 = 0.0556$ and $wR2 = 0.1206$ for 1664 reflections with $I > 2\sigma(I)$.

Molecular orbital shapes in Fig. 4–6, S3, S4, S6 and S8 (ESI†) were established *via* single-point HF/6-311G* calculations with Gaussian 98 using the Cube = (55,Orbital) option.[30] Atomic coordinates for these calculations were taken from the experimental (X-ray) structures of tetracyanopyrazine π-dimer. Energy dependence in Fig. 4 was obtained *via* single-point Gaussian 98 (HF/6-311G*) computations of the artificial dimer structures in which two planar **TCP** monomers were arranged cofacially atop each other with different twist angle ϕ (from 0 to 60°) at interplanar separation of 3.2 Å. The reference point, $E^0 = 0$, in Fig. 4 represents the energy of the dimer consisting of the monomers with parallel N–N axes (*i.e.* $\phi = 0$). It should be noted that (a) DFT (B3LYP/6-311G*) computations of the molecular orbital shapes and energy dependence on rotation afforded very similar results; (b) the rigorous computations of the dimer energetics (relative to the isolated monomers) requires accounting for the electrostatic forces and dispersion, as described earlier in high-level MRMP2,[20a] MCQDPT/CASSCF[20b,c], *etc.*, computations of π-dimers of tetracyanoethylene and cyanil anion-radicals.

Acknowledgements

We thank J. H. Kim for the preparation and S. V. Lindeman for the X-ray measurements of [**BP**, **TCP**] crystals, T. Y. Rosokha for crystallization of [**TTF**, **TCP**], I. S. Neretin for X-ray measurements of [K(L)(THF)$_2$]**TCP**, and the R. A. Welch Foundation and National Science Foundation for financial support.

References

1 (*a*) J. Ferraris, D. O. Cowan, V. Walatka and J. H. Perlstein, *J. Am. Chem. Soc.*, 1973, **95**, 948; (*b*) L. B. Coleman, M. J. Cohen, D. J. Sandman, F. G. Yamagishi, A. F. Garito and A. J. Heeger, *Solid State Commun.*, 1973, **12**, 1125; (*c*) J. R. Ferraro and J. M. Williams, *Introduction to Synthetic Electrical Conductors*, Academic, Orlando, FL, 1987.
2 (*a*) J. S. Miller, P. J. Krusic, A. J. Epstein, W. M. Reiff and J. H. Zhang, *Mol. Cryst. Liq. Cryst.*, 1985, **120**, 27; (*b*) J. S. Miller, *Inorg. Chem.*, 2000, **39**, 4392.
3 (*a*) V. Khodorkovsky and J. Y. Becker, in *Organic Conductors: Fundamentals and Applications*, ed. J.-P. Farges, Marcel Dekker, NY, 1994; (*b*) See also: V. Khodorkovsky and J. Y. Becker, *Chem. Rev.*, 2004, **104**(11), *Molecular Conductors (Thematic Issue)*, Guest Ed. P. Batail.
4 J. S. Miller and M. Drillon, *Magnetism: Molecules to Materials*, Wiley-VCH, Weinheim, 2005.
5 (*a*) J. S. Miller and J. J. Novoa, *Acc. Chem. Res.*, 2007, **40**, 189; (*b*) J. J. Novoa, P. Lafuente, R. E. Del Sesto and J. S. Miller, *Angew. Chem., Int. Ed.*, 2001, **40**, 2540; (*c*) R. E. Del Sesto, J. S. Miller, P. Lafuente and J. J. Novoa, *Chem. Eur. J.*, 2002, **8**, 4894.
6 (*a*) S. V. Rosokha and J. K. Kochi, *Acc. Chem. Res.*, 2008, **41**, 641; (*b*) S. V. Rosokha and J. K. Kochi, *J. Am. Chem. Soc.*, 2007, **129**, 3683.
7 (*a*) J.-M. Lü, S. V. Rosokha and J. K. Kochi, *J. Am. Chem. Soc.*, 2003, **125**, 12161; (*b*) S. V. Rosokha and J. K. Kochi, *J. Am. Chem. Soc.*, 2007, **129**, 828; (*c*) S. V. Rosokha, J.-J. Lu, T. Y. Rosokha and J. K. Kochi, *Phys. Chem. Chem. Phys.*, 2008, DOI: 10.1039/b811816g.
8 (*a*) D. Yamazaki, T. Mishinaga, N. Tanino and K. Komatsu, *J. Am. Chem. Soc.*, 2006, **128**, 14470; (*b*) T. Nishinaga and K. Komatsu, *Org. Biomol. Chem.*, 2005, **3**, 561.
9 (*a*) D. Small, V. Zaitsev, Y. Jung, S. V. Rosokha, M. Head-Gordon and J. K. Kochi, *J. Am. Chem. Soc.*, 2005, **127**, 7411; (*b*) X. Chi, F. S. Tham, A. W. Cordes, M. E. Itkis and R. C. Haddon, *Synth. Met.*, 2003, **133–134**, 367.
10 (*a*) J. S. Huang and M. Kertesz, *J. Phys. Chem. A*, 2007, **111**, 6304; (*b*) J. Huang, S. Kingsbury and M. Kertesz, *Phys. Chem. Chem. Phys.*, 2008, **10**, 2625; (*c*) J. Huang and M. Kertesz, *J. Am. Chem. Soc.*, 2007, **129**, 1634.
11 M. Moscherosch, E. Waldhoer, H. Binder, W. Kaim and J. Fiedler, *Inorg. Chem.*, 1995, **34**, 4326.
12 S. Fukuzumi and J. K. Kochi, *J. Org. Chem.*, 1981, **46**, 4116.
13 E. B. Vickers, T. D. Selby and J. S. Miller, *J. Am. Chem. Soc.*, 2004, **126**, 3716.
14 (*a*) Y. S. Rosokha, S. V. Lindeman, S. V. Rosokha and J. K. Kochi, *Angew. Chem., Int. Ed.*, 2004, **43**, 4650; (*b*) B. Han, J.-J. Lu and J. K. Kochi, *Cryst. Growth Des.*, 2008, **8**, 1327.
15 (*a*) J. M. Lu, S. V. Rosokha, S. V. Lindeman, I. S. Neretin and J. K. Kochi, *J. Am. Chem. Soc.*, 2005, **127**, 1797; (*b*) J. M. Lu, S. V. Rosokha, I. S. Neretin and J. K. Kochi, *J. Am. Chem. Soc.*, 2006, **128**, 16708.
16 (*a*) J. D. Bagnato, W. W. Shum, M. Strohmeier, D. M. Grant, A. M. Arif and J. S. Miller, *Angew. Chem., Int. Ed.*, 2006, **45**, 5322; (*b*) K. I. Pokhodnia, J. Papavassiliou, P. Umek, A. Omerzu and D. Mihailic, *J. Chem. Phys.*, 1999, **110**, 7962.
17 (*a*) D. A. Clemente and A. Marzotto, *J. Mater. Chem.*, 1996, **6**, 941; (*b*) T. C. Umland, S. Allie, T. Kuhlmann and P. Coppens, *J. Phys. Chem.*, 1988, **92**, 6456.
18 T. Devic, M. Yuan, J. Adams, D. C. Fredrickson, S. Lee and D. Venkataraman, *J. Am. Chem. Soc.*, 2005, **127**, 14616.
19 (*a*) K. Goto, T. Kubo, K. Yamamoto, K. Nakasuji, K. Sato, D. Shiomi, T. Takui, M. Kubota, T. Kobayashi, K. Yakusi and J. Ouyang, *J. Am. Chem. Soc.*, 1999, **121**, 1619; (*b*) D. Small, V. Zaitsev, Y. Jung, S. V. Rosokha, M. Head-Gordon and J. K. Kochi, *J. Am. Chem. Soc.*, 2005, **127**, 7411.
20 (*a*) Y. Jung and M. Head-Gordon, *Phys. Chem. Chem. Phys.*, 2004, **6**, 2008; (*b*) I. Garcia-Yoldi, F. Mota and J. J. Novoa, *J. Comput. Chem.*, 2007, **28**, 326; (*c*) Garsia-Yoldi, J. S. Miller and J. J. Novoa, *Phys. Chem. Chem. Phys.*, 2008, **10**, 4106.
21 (*a*) R. B. Woodward and R. Hoffmann, *Angew. Chem., Int. Ed. Engl.*, 1969, **8**, 781; (*b*) I. Fleming, *Frontier Orbitals and Organic*

Chemical Reactions, Wiley & Sons, London, 1975; (*c*) V. F. Traven, *Frontier Orbitals and Properties of Organic Molecules*, Ellis Horwood, New York, 1992.
22 (*a*) H. P. Fritz, H. Gebauer, P. Friedrich, P. Ecker, R. Artes and U. Schubert, *Z. Naturforsch., B: Anorg. Chem., Org. Chem.*, 1978, **33**, 498; (*b*) V. Enkelmann, B. S. Morra, C. Krohnke, G. Wegner and J. Heinze, *Chem. Phys.*, 1982, **66**, 303.
23 S. V. Rosokha, J.-J. Lu, T. Y. Rosokha and J. K. Kochi, *Acta Crystallogr., Sect. C*, 2007, **63**, o347.
24 Note that: (*a*) in general, the formation of the dianionic $(\mathbf{TCP})_2^{2-}$ dimers involves dispersion and electrostatics interactions, which represent critical components of the long-distance π-bonding of ion-radicals,[19,20] and rigorous evaluation of the dimer energetics (relative to the separated monomers) and its bonding components is deferred herein; (*b*) The molecular orbital shape in Fig. 3 is shown with the isosurface function value au (−3/2) (boundary density) of 0.02. The decrease of this value to 0.005 reveals additional weak bonding between two pairs of terminus nitrogens (Fig. S8 in ESI†); (*c*) Note that the π-bonding in $(\mathbf{TCP})_2^{2-}$ dimers occurs between the *delocalized* orbitals of the monomers, which hinders its interpretation as "multiple C–C bonding".[5]
25 S. V. Rosokha and J. K. Kochi, *J. Org. Chem.*, 2006, **71**, 9357.
26 (*a*) For example, the bond length differences between monomeric and π-bonded moieties of octamethylanthracene, *p*-chloranil, dichlorodicyano-*p*-benzoquinone and tetrathiafulvalene ion-radicals are mostly within the accuracy limit of the X-ray measurements; (*b*) Note, that the values of the central C=C bond lengths measured in eight different π-dimerized anion-radical salts of $TCNE^{-\bullet}$ vary in the range: 1.41 to 1.45 Å, and in five salts of monomeric anion radicals they vary from 1.385 to 1.413 Å. The average value of dimerized species is thus somewhat higher than monomeric analogues. However, the most reliable neutron diffraction measurements reveal essentially the same values in dimerized and in the monomeric anion-radical $TCNE^{-\bullet}$ *i.e.* 1.424(4) and 1.429 Å, respectively, see: J. S. Miller, *Angew. Chem., Int. Ed.*, 2006, **45**, 2508.
27 R. S. Mulliken and W. B. Person, *Molecular Complexes*, Wiley, New York, 1969.
28 (*a*) S. V. Rosokha, D. Sun and J. K. Kochi, *J. Phys. Chem. B*, 2007, **111**, 6555; (*b*) S. V. Rosokha, S. M. Dibrov, T. Y. Rosokha and J. K. Kochi, *Photochem. Photobiol. Sci.*, 2006, **5**, 914; (*c*) S. V. Rosokha and J. K. Kochi, *J. Am. Chem. Soc.*, 2001, **123**, 8985.
29 (*a*) G. M. Sheldrick, *SADABS (Ver. 2.03)*, 2000; (*b*) G. M. Sheldrick, *SHELXS 97*, University of Göttingen, Germany, 1997.
30 J. A. Pople, *et al.*, *Gaussian 98, Revision A.11.3 ed.*, Gaussian, Inc., Pittsburgh, PA, 1998.